

Analytical Methods

Accepted Manuscript



This is an *Accepted Manuscript*, which has been through the Royal Society of Chemistry peer review process and has been accepted for publication.

Accepted Manuscripts are published online shortly after acceptance, before technical editing, formatting and proof reading. Using this free service, authors can make their results available to the community, in citable form, before we publish the edited article. We will replace this *Accepted Manuscript* with the edited and formatted *Advance Article* as soon as it is available.

You can find more information about *Accepted Manuscripts* in the [Information for Authors](#).

Please note that technical editing may introduce minor changes to the text and/or graphics, which may alter content. The journal's standard [Terms & Conditions](#) and the [Ethical guidelines](#) still apply. In no event shall the Royal Society of Chemistry be held responsible for any errors or omissions in this *Accepted Manuscript* or any consequences arising from the use of any information it contains.

1
2
3
4 **1 Enhanced chemiluminescence of the luminol-hydrogen peroxide system by**
5
6 **2 BSA-stabilized Au nanoclusters as peroxidase mimic and its application**
7
8

9 3

10
11 **4 Mao Deng, Funan Chen* and Shuangjiao Xu**
12

13 5

14
15
16 6 The Key Laboratory of Luminescence and Real-time Analysis, Ministry of Education;
17
18 7 School of Chemistry and Chemical Engineering, Southwest University, Chongqing,
19
20
21 8 China 400715
22

23 9

24
25
26 **10 Contact information for Corresponding Author**
27

28
29 11 Associate Professor Funan Chen, School of Chemistry and Chemical Engineering,
30
31 12 Southwest University, Chongqing, 400715, P.R. China
32
33 13 Fax: 86-23-68258363. Tel: +86-13752919874
34
35
36 14 E-mail: chenfn@swu.edu.cn
37

38 15

39 16

40 17

41 18

42 19

43 20

44 21

45 22
46
47
48
49
50
51
52
53
54
55
56
57
58
59
60

1
2
3
4 23 **Abstract**
5
6 24
7
8
9 25 In the present work, water-soluble Au nanoclusters capped with Bovine serum albumine
10
11 26 (BSA) was synthesized. It was found that as a peroxidase mimic, Au nanoclusters could
12
13 27 enhance the chemiluminescence (CL) emission from the luminol-hydrogen peroxide
14
15 28 system in alkaline medium, and the enhancement mechanism of Au nanoclusters on
16
17 29 luminol CL was discussed. The effects of the reactant concentrations and some organic
18
19 30 compounds were also investigated. The proposed method could be used as a sensitive
20
21 31 detection tool for hydrogen peroxide and glucose.
22
23
24
25
26 32
27
28
29 33 **Keywords**
30
31 34 chemiluminescence; Au nanoclusters; peroxidase mimic; luminol; glucose
32
33
34 35
35
36 36
37
38
39 37
40
41 38
42
43 39
44
45
46 40
47
48
49 41
50
51 42
52
53 43
54
55
56 44
57
58
59
60

In the present work, water-soluble Au nanoclusters capped with Bovine serum albumine (BSA) was synthesized. It was found that as a peroxidase mimic, Au nanoclusters could enhance the chemiluminescence (CL) emission from the luminol-hydrogen peroxide system in alkaline medium, and the enhancement mechanism of Au nanoclusters on luminol CL was discussed. The effects of the reactant concentrations and some organic compounds were also investigated. The proposed method could be used as a sensitive detection tool for hydrogen peroxide and glucose.

Keywords

chemiluminescence; Au nanoclusters; peroxidase mimic; luminol; glucose

1. Introduction

Chemiluminescence (CL) is light emission produced in a chemical reaction from the decay of chemiexcited species to the electronic ground state [1]. CL and related analytical techniques have attracted extensive interest since the CL phenomenon of luminol was first reported by Albrech [2], owing to its extremely high sensitivity along with its other advantages, such as simple instrumentation, wide calibration ranges, and suitability for miniaturization in analytical chemistry [3-6]. CL has been developed as important and powerful tools in different fields (e.g., environmental analysis, pharmaceutical analysis, food analysis, bioanalysis and immunoassay) [7-11].

Though CL has been investigated for years, study of CL was limited to some molecular systems. In recent years, much attention has been extended to the CL of nanomaterial systems, to improve the sensitivity and the stability. Many investigations have indicated that use of nanoparticles in CL reactions has provided new avenues to enhance the inherent sensitivity and expand new applications of this mode of detection [12]. Li et al. found that CeO₂ nanoparticles could enhance the CL emission of luminol-H₂O₂ system and developed a specific sandwich assay for human α -thrombin [13]. Chen et al. have made use of the active catalysis of the CuO nanoparticles to detect glucose and cholesterol [14-15]. Wei et al. reported that the chemiluminescence of the luminol-H₂O₂ system could be enhanced by ZnO nanoparticles [16]. In other cases, Cui and co-workers have reported many prominent works about noble metal nanoparticles-catalyzed CL systems, such as Au, Ag, and Pt nanoparticles, which significantly improved the inherent sensitivity and selectivity of the

1
2
3
4 67 traditional CL systems [17-19].
5

6 68 Au nanoclusters (Au NCs), owing to their ultrasmall size, biocompatibility, nontoxicity
7
8
9 69 and highly fluorescent properties, have drawn wide attention [20-22]. Recently, these
10
11 70 protein-templated Au NCs have been successfully applied to cancer-cell imaging [23],
12
13 71 tumor imaging in vivo [24], and Hg^{2+} , CN^- , Cu^{2+} and H_2O_2 detection [25-28] and so forth.
14
15
16 72 Wang et al. demonstrated that bovine serum albumin (BSA) stabilized Au clusters exhibited
17
18
19 73 highly intrinsic peroxidase-like activity firstly [29]. Compared with other reported
20
21 74 nanoparticles as peroxidases mimetics, BSA-Au clusters possess intrinsic peroxidase-like
22
23 75 activity and have effective enzyme-like catalysis over a wide range of temperatures and pH
24
25
26 76 values compared with nature enzymes [29-30]. However, there are no reports exploring the
27
28
29 77 catalytic property of Au NCs in the luminol CL reactions, to the best of our knowledge.

30
31 78 Luminol is one of the earliest and most common CL reagents used in CL reaction. The
32
33
34 79 luminol- H_2O_2 system still plays an important role in modern chemical analysis [31-35]. In
35
36
37 80 the present study, Au NCs, the novel classes of intermediates between noble-metal atoms
38
39 81 and nanoparticles materials, were chosen as catalysts for the luminol CL system and
40
41 82 explored the effect of colloidal solutions of Au NCs on the CL for the first time. The
42
43
44 83 possible enhancement of Au NCs mechanism was investigated. Based on the effect of Au
45
46 84 NCs on the luminol- H_2O_2 CL system, the feasibility of using the proposed method for H_2O_2
47
48
49 85 and glucose detection was studied. Under optimum conditions, the CL intensity was linear
50
51 86 with H_2O_2 concentration. In this work, we established a simple, low-cost sensor for glucose
52
53
54 87 by coupling the highly selective enzymatic procedure with the sensitive
55
56 88 chemiluminescence reaction catalyzed by Au NCs successfully.
57
58
59
60

1
2
3
4 89 **2. Experimental**
5
6

7 90
8

9 91 *2.1 Reagents and materials*
10

11 92 Bovine serum albumin (BSA), Glucose oxidase (GOx) and Glucose were purchased
12 from Sangon Biotech Co., Ltd. (Shanghai, China). $\text{HAuCl}_4 \cdot 3\text{H}_2\text{O}$ and sodium borohydride
13 93 were purchased from Sinopharm Chemical Reagent Co., Ltd. (Shanghai, China). 30% (v/v)
14 94 H_2O_2 and sodium hydroxide were purchased from Kelong Reagent Co., Chengdu, China.
15 95

16 96 A 1.0×10^{-2} mol/L stock solution of luminol (3-aminophthalhydrazide) was prepared by
17 97 dissolving luminol (Sigma) in 0.1 mol/L sodium hydroxide solutions. Working solutions of
18 98 luminol were prepared by diluting the stock solution. Working solutions of H_2O_2 were
19 99 prepared fresh daily by dilution of 30% (v/v) H_2O_2 . Clinical serum samples were provided
20 100 by the three gorges central hospital of Chongqing. All chemicals and reagents were of
21 101 analytical grade and used without further purification, and ultrapure water was used
22 102 throughout.
23 103
24 104

25 105
26 106
27 107
28 108
29 109
30 110
31
32
33
34
35
36
37
38
39
40
41 104 *2.2 Instrumentation*
42

43 105 Batch model BPCL ultra weak chemiluminescence analyzer (Institute of Biophysics,
44 106 Chinese Academy of Sciences, Beijing, China) was employed to study the characteristics of
45 107 the CL reaction. The CL detection was conducted on a flow injection chemiluminescence
46 108 system comprising of a peristaltic pump (Ruimai Company Xi'an, China), PTFE tubing
47 109 (0.8 mm i.d.) which was used as connection material in the flow system. Data acquisition
48 110 and treatment were performed with BPCL software running under Windows XP. The CL
49
50
51
52
53
54
55
56
57
58
59
60

1
2
3
4 111 spectra were obtained with an F-4500 spectrofluorimeter (Hitachi, Japan) under the model
5
6 112 of fluorescence scan by turning off the excitation light. The pH of the solutions was
7
8 113 detected by a PHS-3C precision pH meter (Shanghai Precision Scientific Instruments Co.,
9
10 114 Ltd., China). UV-vis absorption spectra were achieved with a Model UV-2550s
11
12 115 Spectrophotometer (Shimadzu, Japan).
13
14
15
16
17

117 *2.3 Synthesis of BSA-Au nanoclusters and BSA-Au nanoparticles*

118 *2.3.1 Synthesis of BSA-Au nanoclusters*

119 BSA modified Au NCs was synthesized in aqueous solution following a previous
120 publication with minor modifications [36]. In a typical experiment, All glassware was
121 washed with AquaRegia (HCl: HNO₃ volume ratio = 3:1), and rinsed with ethanol and
122 ultrapure water. 15 mL aqueous HAuCl₄ solution (10 mmol/L, 37°C) was added to BSA
123 solution (15 mL, 50 mg/mL, 37°C) under magnetic stirring. Then, 1.5 mL 1mol/L NaOH
124 solution was introduced and the mixture was allowed to incubate at 37°C under vigorous
125 stirring for 24 h. The color of the solution changed from light yellow to light brown, and
126 then to deep brown. The solution was then dialyzed in double distilled water for 48 h to
127 remove unreacted HAuCl₄ or NaOH. The final solution was stored at 4°C in refrigerator
128 when not in use. The UV-vis and fluorescence spectra of as-prepared Au NCs are shown in
129 Figure S2 and S3. Upon being excited 470 nm, the Au NCs showed an emission band
130 centered at 640 nm. The features of the obtained spectra are consistent with previous
131 studies [36].

132 *2.3.2 Synthesis of BSA-Au nanoparticles*

1
2
3
4 133 Au NPs were prepared according to the Liu's method [37]. In brief, 0.6700 g of BSA and
5
6 134 0.0125 g of $\text{HAuCl}_4 \cdot 4\text{H}_2\text{O}$ was dissolved in 100 mL of ultra-pure water, the obtained
7
8
9 135 yellow solution was stirred more than 2 h. And then, 0.1530 g of NaBH_4 was slowly added
10
11 136 into this solution with rapid stirring for 3 h. At last, the product was purified through
12
13 137 centrifugation (11 000 rpm) to remove the large gold nanoparticles, leaving a clear, dark
14
15
16 138 red BSA-protected gold nanoparticles solution. The UV-vis spectra of as -prepare Au NPs
17
18
19 139 are shown in Figure S1.

20 21 140 *2.4 General procedure for CL analysis*

22
23 141 The CL intensity was measured by a flow injection CL system. The flow system
24
25 142 employed consisted of two peristaltic pumps. One delivered luminol and Au NCs at a flow
26
27 143 rate (per tube) of 0.8 mL/min. The other delivered the sample and carrier stream at the
28
29 144 same flow rate. PTFE tubing (0.8 mm i.d.) was used to connect all components in the flow
30
31 145 system. Injection was made using a six-way injection valve equipped with an eight cm
32
33 146 length sampling loop. The CL signal produced was detected by a photomultiplier tube
34
35 147 (operated at -550 V), and was then recorded by a computer equipped with a data
36
37 148 acquisition interface. Data acquisition and treatment were performed with BPCL software
38
39 149 running under Windows XP.

40
41 150 For characterization of the chemiluminescent analysis system, aqueous standards were
42
43 151 used. A series of working standard solutions with different concentrations was prepared by
44
45 152 diluting a concentrated fresh standard solution of H_2O_2 or glucose with water. The net CL
46
47 153 emission intensity ($\Delta I = I_1 - I_0$, where I_1 is the CL intensity of the sample solution and I_0
48
49 154 that of the blank solution) versus H_2O_2 concentration was used for the calibration. At each
50
51
52
53
54
55
56
57
58
59
60

1
2
3
4 155 H₂O₂ or glucose concentration, the injection was repeated at least three times, and the
5
6 156 average CL signal was obtained.
7
8

9 157

10 11 158 *2.5 Glucose determination in real serum samples*

12
13
14 159 For glucose determination in blood, the serum samples from a local hospital were
15
16 160 firstly treated by centrifugation at 3000 rpm for 30 mins. Then 0.10 mL of the supernatant
17
18 161 was diluted into 10 mL using 1×10^{-2} mol/L PBS buffer (pH 7.0) for the following work.
19
20
21 162 Glucose determination was carried out by adding 0.1 mL of the diluted serum sample and
22
23 163 0.1 mL of 1 mg/mL GOx in 0.50 mL of 10 m mol/L PBS buffer (pH 7.0), the mixture was
24
25 164 incubated at 37 °C for 30 mins, and then the resulting mixture was diluted to 10 mL by
26
27 165 1×10^{-2} mol/L PBS buffer solution (pH 7.0), and then used for glucose determination. The
28
29 166 calibration curve for glucose detection was realized as follows: (a) 0.1 mL of 1 mg/mL
30
31 167 GOx and 0.1 mL of glucose of different concentrations in 0.50 mL of 1×10^{-2} mol/L M PBS
32
33 168 buffer (pH 7.0) were incubated at 37 °C for 30 mins, then the resulting solutions were
34
35 169 diluted to 10 mL with 1×10^{-2} mol/L PBS buffer , leading to the final glucose concentration
36
37 170 of 0.05– 10×10^{-6} mol/L; (b) the produced mixed solution was used to prepare the calibration
38
39 171 curve for glucose by the proposed CL method. The results were compared with those by the
40
41 172 conventional method. The comparison study was carried out by a One Touch Ultra glucose
42
43 173 meter (Johnson and Johnson Medical Ltd., Shanghai, China). All experiments on glucose
44
45 174 analysis in blood were performed in compliance with the relevant laws and institutional
46
47 175 guidelines.
48
49
50
51
52
53
54
55
56
57
58
59
60

1
2
3
4 177 **3. Results and discussion**

5
6 178

7
8
9 179 *3.1 Enhancement of luminol CL*

10
11 180 In alkaline media, the oxidation of luminol by H₂O₂ generates weak CL. Figure 1
12
13 181 shows the kinetic curves of the Au NCs enhanced CL system, which indicated that Au NCs
14
15 182 could highly enhance CL systems. In order to explore the CL enhancing phenomena, the
16
17 183 CL spectra for AuNCs mixed with luminol–H₂O₂ was acquired. Figure 2 is the CL spectra
18
19 184 of luminol–H₂O₂–Au NCs system. The maximal emission was at ~425 nm, revealing that
20
21 185 the luminophor was still the excited state 3-aminophthalate anions. Therefore, the addition
22
23 186 of AuNCs did not lead to the generation of a new luminophor for this CL system. The
24
25 187 enhanced CL signals were thus ascribed to the possible catalysis from AuNCs.
26
27
28
29
30

31 188

32
33 189 *3.2 Optimization of the reaction conditions*

34
35
36 190

37
38
39 191 The reaction conditions were optimized for the luminol–H₂O₂–AuNCs CL system
40
41 192 shown in Figure. 3. The pH of luminol solution played an important role in the CL reaction.
42
43 193 The effect of pH on the CL was studied in the range of pH 10.0–12.5. The experimental
44
45 194 results in Figure.3a indicated that the maximum CL intensity was obtained at pH 11.3 in
46
47 195 sodium hydroxide solution. When the pH of luminol solution was lower than 11.3, the CL
48
49 196 intensity increased with increasing the pH. When the pH of luminol solution was higher
50
51 197 than 11.3, the CL intensity decreased with increasing the pH. The effect of luminol
52
53 198 concentration on the CL was studied in the range from 1.0×10^{-5} to 3.5×10^{-5} mol/L. The
54
55
56
57
58
59
60

1
2
3
4 199 result is shown in Figure.3b. As can be seen, the CL intensity increased with increasing
5
6 200 luminol concentration in the range of 1.0×10^{-5} to 2.7×10^{-5} mol/L. An increase of the CL
7
8 201 signal intensity was observed when the concentration of luminol was lower than 2.7×10^{-5}
9
10
11 202 mol/L. However, when the concentration of luminol was above 2.7×10^{-5} mol/L, only
12
13 203 slight changes in the light intensity were observed. Therefore, 2.7×10^{-5} mol/L was chosen
14
15 204 as the optimal luminol concentration in the present study. Different concentrations of Au
16
17 205 NCs were added to the CL system, they enhanced the CL intensity in different degrees. The
18
19 206 effect of Au NCs concentration was investigated over the range 4.0–20.0 mg/L (Figure 3c).
20
21 207 It was found that the maximum CL intensity was obtained at 16.0 mg/L, above which the
22
23 208 CL intensity decreased, probably due to the self-absorption of the emission by Au NCs.
24
25 209 Therefore, 16.0 mg/L of Au NCs was chosen for the next experiments.
26
27
28
29
30
31
32

33 211 *3.3 Mechanism Discussion*

34
35
36 212 The CL-generation mechanism for luminol oxidation in aqueous solution has been
37
38 213 extensively studied. Merényi et al. had summarized the major CL-generating mechanism
39
40 214 for luminol oxidation in aqueous solution to occur in three basic steps, as shown in Scheme
41
42 215 1: (1) oxidation of luminol to the luminol radical; (2) oxidation of the luminol radical to
43
44 216 hydroxy hydroperoxide, the key intermediate; (3) decomposition of hydroxyl
45
46 217 hydroperoxide with or without the emission of CL, among which step 1 was supposed to be
47
48 218 the rate-determining step of luminol CL [38–39]. The presence of oxygen-related radicals
49
50 219 (for example, $\text{OH}\cdot$, $\text{O}_2^{\cdot-}$, and other radical derivatives) as oxidants was expected to occur,
51
52 220 during the luminol oxidation processes. As for the luminol– H_2O_2 system, the CL reaction
53
54
55
56
57
58
59
60

1
2
3
4 221 of superoxide radical with luminol in alkaline solution was catalyzed in the presence of
5
6 222 H₂O₂.

7
8
9 223 In order to explore the possible mechanism, the UV-visible absorption spectra were
10
11 224 recorded. As shown in Figure. 4, it could be seen that Au NCs had no maximum absorption
12
13 225 peak in the ranges 280–600 nm, and the luminol–H₂O₂ system had two absorption peaks at
14
15 226 304 and 346 nm. When mixed with luminol–H₂O₂ system, the UV-visible peak was not
16
17 227 changed, indicating no change occurred after the reaction. Therefore, the enhancement of
18
19 228 CL signals may have originated from the catalytic effects of Au NCs.

20
21
22
23
24 229 Based on the above discussion, it can be concluded that when added in the
25
26 230 luminol-hydrogen peroxide system, Au NCs may interact with the reactants or the
27
28 231 intermediates of the reaction of luminol with hydrogen peroxide. It is possible that AuNCs
29
30 232 as the catalysts could catalyze the decomposition of H₂O₂ to yield active intermediates such
31
32 233 as OH•, O₂^{•-}. The hydroxyl radical reacted with luminol to form luminol radical (L^{•-}), then
33
34 234 the produced L^{•-} reacts with superoxide anion, yielding an unstable endoperoxide and an
35
36 235 electronically excited 3-aminophthalate anion (3-APA*), leading to enhanced light
37
38 236 emission shown in Scheme 2.

39
40
41
42
43
44 237 In order to prove the correctness of the mechanism, we investigated the effect on CL
45
46 238 of luminol in the presence of Au NPs @BSA and Au NCs@BSA. As shown in Figure5, the
47
48 239 CL intensity was enhanced greatly by Au NCs, probably because that quantum size effects
49
50 240 began to function with an increase in band gap energy, leading to a higher activation energy
51
52 241 that was needed for electron transfer, which would be disadvantageous for the partial
53
54 242 electron transfer from Au NPs to H₂O₂, and then decrease the catalytic efficiency of Au
55
56
57
58
59
60

1
2
3
4 243 NPs for luminol CL reaction [40].
5
6
7

8
9
10
11 244

12
13
14
15 245

16 246 *3.4 Inhibition effects of organic compounds*

17
18
19
20
21
22
23
24
25
26
27
28
29
30
31
32
33
34
35
36
37
38
39
40
41
42
43
44
45
46
47
48
49
50
51
52
53
54
55
56
57
58
59
60

247 Organic compounds containing hydroxyl (OH), amino (NH₂), or mercapto (SH) groups
248 have been reported to compete with luminol for active oxygen intermediates, leading to a
249 decrease in CL intensity. On the other hand, these compounds may interact with AuNCs to
250 reduce the active surface area, interrupting the formation of luminol radicals and hydroxyl
251 radicals taking place on the surface of nanoparticles. Therefore, the effects of such organic
252 compounds on the CL system were investigated. The results are listed in Table 1. As is
253 expected, all the tested compounds with the concentration of 1×10^{-5} g/mL inhibited the CL
254 signal of the luminol–H₂O₂–Au NCs system. The results demonstrate that the
255 luminol–H₂O₂–Au NCs system system has a wide application for the determination of such
256 compounds. However, the usefulness of this technique in terms of selectivity may be
257 limited. If it combined with separation techniques, this CL detection will not be
258 problematic. Therefore, it is ideal for the design of a CL detector in HPLC and
259 high-performance capillary electrophoresis by use of this CL system for the simultaneous
260 detection of numerous compounds.

261 *3.5 Analytical applications*

262 Under the optimum conditions described above, the calibration graph of the relative CL
263 intensity versus H₂O₂ concentration was linear in the range from 2.0×10^{-8} to 5.0×10^{-6}
264 mol/L Figure 6. The limit of detection (LOD) for H₂O₂ was 6.0×10^{-9} mol/L. The RSD of

1
2
3
4 265 the method was 3.86% for 1.0×10^{-7} mol/L H_2O_2 ($n = 7$). The regression equation is ΔI
5
6 266 $=850.09+1624.99 [\text{H}_2\text{O}_2]$ (μM), $R^2 = 0.9969$ ($n = 7$).

7
8
9 267 Because H_2O_2 is the main product of the glucose oxidase (GOx)-catalyzed reaction,
10
11 268 therefore, when combined with glucose oxidase (GOx), the proposed CL method could be
12
13 269 used for the determination of glucose, which is an important indicator for the diagnosis of
14
15 270 diabetes mellitus in clinical medicine. The linear range for glucose was from 5.0×10^{-7} to
16
17 271 1.0×10^{-5} mol/L and the limit of detection was 1×10^{-7} mol/L (Figure.7). The RSD was
18
19 272 2.2% for 5.0×10^{-6} mol/L glucose ($n = 7$). The regression equation is $\Delta I =527.54+383.77$
20
21 273 $[\text{glucose}]$ (μM), $R^2 = 0.9957$ ($n = 7$). The present method was compared to the analytical
22
23 274 methods previously published in the literature [14, 34, 41–44] using the luminol- H_2O_2 CL
24
25 275 system for H_2O_2 and glucose analysis in terms of LODs (the detection limits). The LODs
26
27 276 are listed in Table 2. As can be seen, the proposed method shows high sensitivity for H_2O_2
28
29 277 and glucose analysis.

30
31
32
33
34
35
36 278 The selectivity of the proposed method was also studied. The selectivity experiments
37
38 279 were carried out by using a series of solutions containing 5×10^{-6} mol/L glucose plus
39
40 280 various amounts of maltose, lactose, fructose or sucrose. It was found that negligible CL
41
42 281 change was observed even after adding 5×10^{-6} mol/L maltose, lactose, fructose or sucrose.
43
44 282 This indicates that the present biosensing system has high selectivity for glucose.

45
46
47
48
49 283 To evaluate the feasibility of the sensing system for analysis of glucose in biological
50
51 284 samples, the proposed method was used to detect glucose in blood samples, and the results
52
53 285 were compared with those obtained by the conventional method. The comparison study
54
55 286 was carried out by a One-Touch Ultra glucose meter (Johnson and Johnson Medical Ltd.,
56
57
58
59
60

1
2
3
4 287 Shanghai, China). The detailed procedure is described in the Experimental section. The
5
6 288 results are listed in Table 3, it can be seen that the results obtained by the proposed method
7
8
9 289 were in good agreement with those measured by glucose oxidase endpoint method. The
10
11 290 practical applicability of the proposed method was further verified through standard
12
13 291 addition experiments, with the recoveries of glucose in three serum samples ranging from
14
15
16 292 96.5% to 102.7%. Therefore, the proposed method is suitable and satisfactory for glucose
17
18
19 293 analysis of real samples.

20
21 294

22 295 **4. Conclusion**

23
24 296 Au NCs were found to enhance the luminol-H₂O₂ CL signals in this work. The
25
26 297 enhancement of CL was suggested to attribute to the peroxidase-like activity of AuNCs,
27
28
29 298 which effectively catalyzed the decomposition of hydrogen peroxide into hydroxyl radicals.
30
31 299 Some organic compounds containing hydroxyl, amino, or mercapto groups were observed
32
33
34 300 to inhibit the CL signals of the luminol-H₂O₂-AuNCs system at the experimental
35
36
37 301 conditions, which could be potentially applied in the analysis of these compounds. In
38
39 302 addition, a novel AuNCs-based enzyme nano-mimic CL method was used successfully for
40
41 303 H₂O₂ and glucose detection. This work is of great benefit to the insight of the enzyme
42
43
44 304 nano-mimics and their potential applications in CL and bioanalysis.

45
46 305

48 306 **Acknowledgement**

49
50
51 307 We thank Prof. H. Z. Zheng and Prof. Y. M. Huang for measurements.
52
53
54 308

55
56 309
57
58
59
60

310

311 **References**312 [1] L. J. Kricka, *Anal. Chem.* 67 (1995) 499–502313 [2] H.O. Albrecht, *Z. Phys. Chem.* 136 (1928), 321–330314 [3] S. Zhao, X. Li, Y. M. Liu, *Anal. Chem.* 81(2009), 3873–3878315 [4] Z. Wang, S. Y. Chin, C. D. Chin, J. Sarik, M. Harper, J. Justman, S. K. Sia, *Anal. Chem.*
316 82 (2010), 36–40317 [5] X. Wang, N. Na, S. C. Zhang, Y. Y. Wu, X. R. Zhang, *J. Am. Chem. Soc.* 129 (2007),
318 6062–6063319 [6] Y. Lv, S. Zhang, G. Liu, M. Huang, X. Zhang, *Anal. Chem.* 77 (2005), 1518–1525320 [7] S. Ahmed, N. Kishikawa, K. Ohyama, T. Maki, H. Kurosaki, K. Nakashima, N. Kuroda.
321 *J. Chromatogr. A* 1216 (2009) 3977–3984322 [8] Q. Xiao, H. F. Li, G. M. Hu, H. R. Wang, Z. J. Li, J. M. Lin, *Clin. Biochem.* 42 (2009)
323 1461–1467324 [9] L. R. Luo, Z. J. Zhang, L. J. Chen, L. F. Ma, *Food Chem.* 97 (2006) 355–360325 [10] M. Yamasuji, T. Shibata, T. Kabashima, M. Kai, *Anal. Biochem.* 413 (2011) 50–54326 [11] F. Chen, S. Mao, H. Zeng, S. Xue, J. Yang, H. Nakajima, J. M. Lin, K. Uchiyama,
327 *Anal. Chem.* 85 (2013) 7413–7418328 [12] Q. Li, L. Zhang, J. Li, C. Lu, *TrAC, Trends Anal. Chem.* 30 (2011) 401–413329 [13] X. Li, L. Sun, A. Ge, Y. Guo, *Chem. Commun.*, 2011, 47, 947–949330 [14] W. Chen, L. Hong, A. Liu, J. Liu, Xi. Lin, X. Xia, *Talanta* 99 (2012) 643–648331 [15] L. Hong, A. Liu, G. Li, W. Chen, X. Lin, *Biosens. Bioelectron.* 43 (2013) 1–5

- 1
2
3
4 332 [16] S. Li, X. Zhang, W. Du, Y. Ni, X. Wei, J. Phys. Chem. C 113 (2009) 1046-1051
5
6 333 [17] Z. Zhang, H. Cui, C. Lai, L. Liu, Anal. Chem. 77 (2005) 3324–3329
7
8 334 [18] J. Z. G. H. Cui, W. Zhou, W. Wang, J. Photochem. Photobiol., A 93 (2008) 89-96
9
10 335 [19] S. L. Xu, H. Cui, Luminescence, 22 (2007) 77-87
11
12 336 [20] Z. Tang, B. Xu, B. Wu, M. W. Germann, G. Wang, J. Am. Chem. Soc. (2010)
13
14 337 3367-3374
15
16 338 [21] Y. Negishi, Y. Takasugi, S. Sato, H. Yao, K. Kimura, T. Tsukuda, Magic-Numbered J.
17
18 339 Am. Chem. Soc., 126 (2004), 6518-6519
19
20 340 [22] H. Lin, L. Li, C. Lei, X. Xu, Z. Nie, M. Guo, Y. Huang, S. Yao, Biosens. Bioelectron.
21
22 341 41 (2013) 256-261
23
24 342 [23] C. L. Liu, H. T. Wu, Y. H. Hsiao, C. W. Lai, C. W. Shih, Y. K. Peng, K. C. Tang, H.
25
26 343 W. Chang, Y. C. Chien, J. K. Hsiao, J. T. Cheng, P. T. Chou, Angew. Chem. Int. Edit.
27
28 344 50 (2011) 7056-7060
29
30 345 [24] X. Wu, X. He, K. Wang, C. Xie, B. Zhou, Z. Qing, Nanoscale, 2 (2010), 2244-2249
31
32 346 [25] W. Chen, X. Tu, X. Guo, Chem. Commun. 13 (2009) 1736-1738
33
34 347 [26] L. Jin, L. Shang, S. Guo, Y. Fang, D. Wen, L. Wang, J. Yin, S. Dong, Biosens.
35
36 348 Bioelectron. 26 (2011) 1965–1969
37
38 349 [27] Y. Liu, K. Ai, X. Cheng, L. Huo, L. Lu, Adv. Funct. Mater. 20 (2010), 951-956
39
40 350 [28] J. Xie, Y. Zheng, J.Y. Ying, Chem. Commun. 46 (2010) 961–963
41
42 351 [29] X. X. Wang, Q. Wu, Z. Shan, Q. M. Huang, Biosens. Bioelectron. 26 (2011)
43
44 352 3614–3619
45
46 353 [30] Y. Tao, Y. Lin, J. Ren, X. Qu, Biosens. Bioelectron. 42 (2013) 41–46
47
48
49
50
51
52
53
54
55
56
57
58
59
60

- 1
2
3
4 354 [31] S. Y. Kazemi, S. M. Abedirad, J. Iran. Chem. Soc. 10 (2013) 251–256
5
6 355 [32] Y. Dong, Z. Wang, J. Chin. Chem. Soc. 60 (2013)108–108
7
8
9 356 [33] P. Yang, S. Y. Jin, Q. Z. Xu, S. H. Yu, Small 9 (2013) 199–204
10
11 357 [34] S. He, W. Shi, X. Zhang, J. Li, Y. Huang, Talanta 82 (2010) 377–383
12
13 358 [35] D. L. Giokas, D. C. Christodouleas, I. Vlachou, A. G. Vlessidis, A. C. Calokerinos,
14
15
16 359 Anal. Chim. Acta 76 (2013) 70–77
17
18
19 360 [36] J. P. Xie, Y. G. Zheng, J. Y. Ying, J. Am. Chem. Soc. 131 (2009) 888–889
20
21 361 [37] L Liu, H. Z. Zheng, Z. J. Zhang, Y. M. Huang, S. M. Chen, Y. F. Hu, Spectrochim.
22
23 362 Acta, Part A 69 (2008) 701-705
24
25
26 363 [38] G. Merényi, J. Lind, T. E. Eriksen, J. Biolumin. Chemilumin., 5 (1990) 53–56
27
28
29 364 [39] T. G. Burdo, W. R. Seitz, Anal. Chem. 47 (1975), 1639–1643
30
31 365 [40] Y. Qi, B. Li. Spectrochim. Acta, Part A 111 (2013) 1–6
32
33 366 [41] L. Luo, Z. Zhang, L. Zhou, Anal. Chim. Acta, 584 (2007) 106–111
34
35
36 367 [42] D. Lan, B. X. Li, Z. J. Zhang, Biosens. Bioelectron., 24(2008) 934–938
37
38
39 368 [43] Y. Zheng, S. L. Zhao, Y. M. Liu, Analyst, 136 (2011) 2890–2892
40
41 369 [44] M. Santafe, B. Doumeche, L. J. Blum, A. P. Girard-Egrot, C. A. Marquette, Anal.
42
43 370 Chem., 82(2010) 2401–2404
44
45
46 371
47
48 372
49
50 373
51
52 374
53
54
55 375
56
57
58
59
60

1
2
3
4 376

5
6 377 **Figure captions:**

7
8
9 378 **Figure1.** Kinetic curves of chemiluminescence systems: (a) luminol-H₂O₂; (b)
10
11 379 luminol-H₂O₂-Au NCs. Luminol: 2.7×10^{-5} mol/L; H₂O₂: 1×10^{-7} mol/L; Au NCs: 5 mg/L.

12
13
14 380

15
16 381 **Figure2.** Chemiluminescence spectra for luminol-H₂O₂-Au NCs system. (a) Au NCs; (b)
17
18 382 luminol-H₂O₂; (c) luminol-H₂O₂-Au NCs. Luminol: 2.7×10^{-5} mol/L; H₂O₂: 1×10^{-7}
19
20 383 mol/L; Au NCs: 5 mg/L; pH 11.3 (sodium hydroxide solution).

21
22
23 384

24
25
26 385 **Figure3.** Effects of the reaction conditions on the luminol-H₂O₂-Au NCs CL system. (a)
27
28 386 Effects of pH of luminol: Luminol: 2.7×10^{-5} mol/L; H₂O₂: 1×10^{-7} mol/L; Au NCs: 5
29
30 387 mg/L (b) Effect of luminol concentration: pH: 11.3; H₂O₂: 1×10^{-7} mol/L; Au NCs: 5 mg/L
31
32 388 (c) Effect of Au NCs: Luminol: 2.7×10^{-5} mol/L; H₂O₂: 1×10^{-7} mol/L; pH: 11.3.

33
34
35 389

36
37
38 390 **Figure4.** UV-visible absorption spectra of (a) Au NCs; (b) luminol-H₂O₂; (c)
39
40 391 luminol-H₂O₂-AuNCs

41
42
43 392

44
45
46 393 **Scheme1.** Schematic CL-generating mechanism for the oxidation of luminol with three
47
48 394 major steps

49
50
51 395

52
53
54 396 **Scheme2.** Possible mechanism for the luminol-H₂O₂-Au NCs CL system.

55
56
57 397

1
2
3
4 398 **Figure5** Comparison of CL intensity in luminol-catalyzed reaction in pH 11.3, 2.7×10^{-5}
5
6 399 mol/L luminol and 1×10^{-7} mol/L H_2O_2 . Inset: Comparison of CL intensity in
7
8
9 400 luminol-catalyzed reaction for Chemiluminescence spectra

10
11 401
12
13 402 **Figure6.** Calibration curves for H_2O_2 . Inset: CL intensity dependence of H_2O_2
14
15 403 concentrations.

16
17
18
19 404
20
21 405 **Figure7.** Calibration curves for glucose. Inset: CL intensity dependence of glucose
22
23 406 concentrations.

24
25
26
27
28
29
30 407
31 408 **Table captions**

32
33 409 **Table 1** Inhibition effects of organic compounds (1.0×10^{-5} mol/L) on luminol- H_2O_2 -Au
34
35 410 NCs CL system.

36
37
38 411 **Table 2** Comparison LOD of this work with some established methods using luminol-based
39
40 412 CL for hydrogen peroxide and glucose

41
42 413 **Table 3** Analytical results of glucose in human serum.

43
44
45 414
46
47 415
48
49 416 **Table 1** Inhibition effects of organic compounds (1.0×10^{-5} mol/L) on luminol- H_2O_2 -Au
50
51
52 417 NCs CL system.

53
54
55 418

Organic compounds	Quenching,a	%	Organic compounds	Quenching,a	%
phenol	82.4		l-histidine	5.1	

catechol	4.7	l-alanine	6.1
phloroglucinol	50.3	l-glutamine	4.9
ascorbic acid	8.4	glycine	6.7
gallic acid	10.0	l-serine	14.3
adrenaline	4.6	l-phenylalanine	12.8
dopamine	25.8	l-cystine	8.9
chlorogenic acid	12.2	glutathione	6.7

a The percentage of quenching was calculated as I/I_0 . The blank CL signal I_0 was obtained by luminol- H_2O_2 -Au NCs CL system without the tested organic compounds

419

420

421 **Table 2** Comparison LOD of this work with some established methods using luminol-based

422

CL for hydrogen peroxide and glucose

System	H_2O_2 (10^{-6} mol/L)	Glucose (10^{-6} mol/L)	Ref
CuO nanoparticles–luminol– H_2O_2	0.01	2.9	14
β -CD/CoFe ₂ O ₄ MNPs–luminol– H_2O_2	0.02		34
Au nanoparticles–Hb/PMMA–luminol– H_2O_2	0.2		41
Gold NPs–luminol– H_2O_2 –HRP		5	42
HRP–MNP–luminol– H_2O_2	0.5	50	43
1-Ethyl-3-methylimidazolium ethylsulfate/ Cu^{2+} –luminol– H_2O_2	5	4	44
Au NCs–luminol– H_2O_2	0.006	0.1	This work

423

424 **Table 3** Analytical results of glucose in human serum (n=3).

samples	Proposed method (10^{-3} mol/L)	Glucose meter (10^{-3} mol/L)
---------	---------------------------------------	-------------------------------------

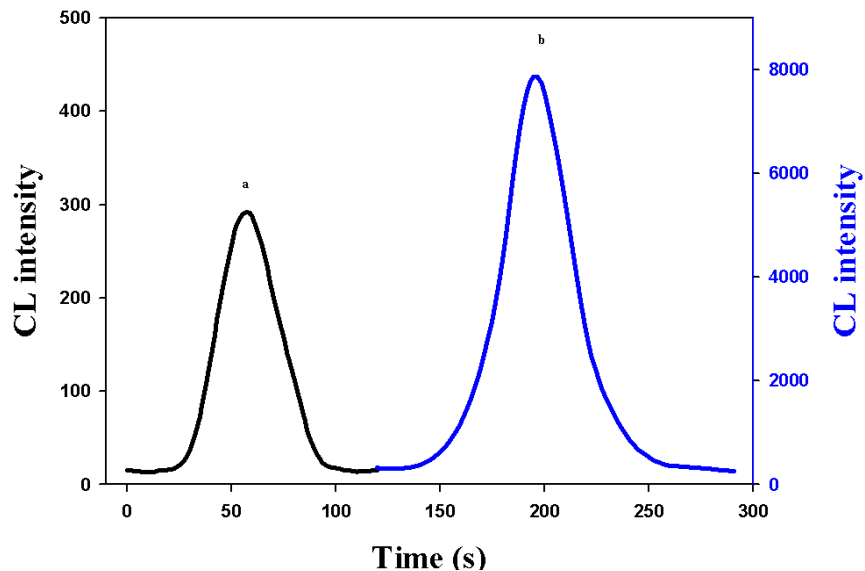
Serum1	0.43±0.01	0.46
Serum2	0.84±0.02	0.85
Serum3	1.12±0.01	1.09

425

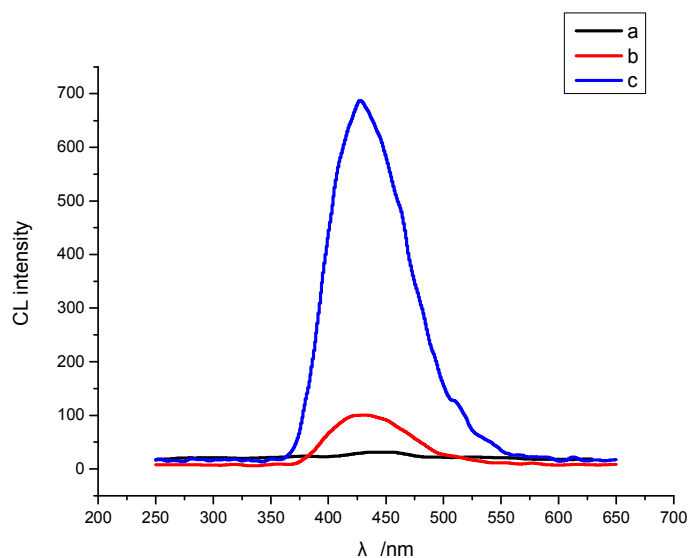
426

427

428



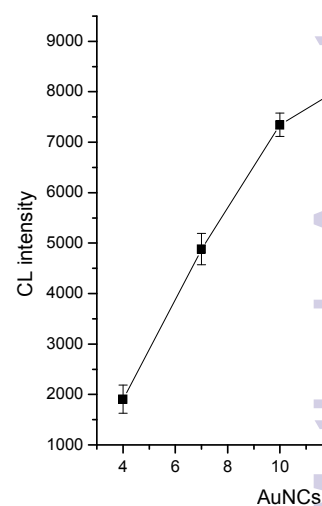
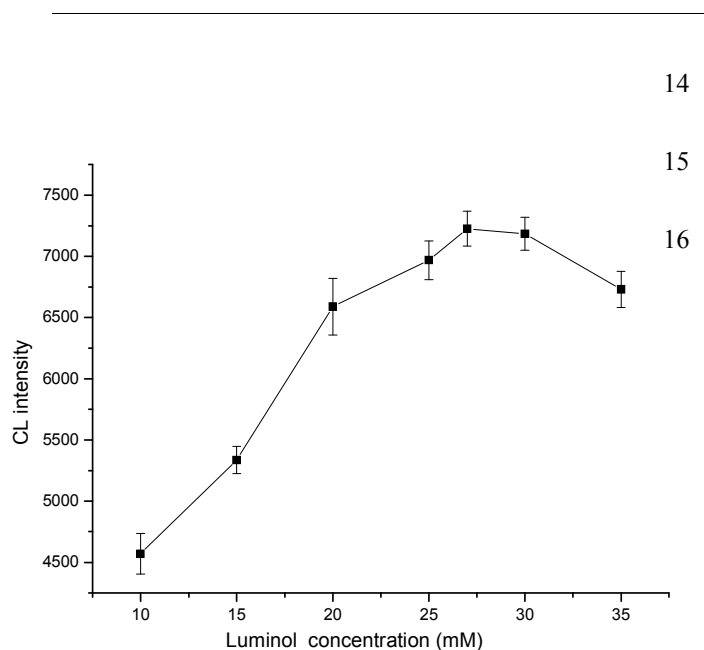
2
3 **Figure1.** Kinetic curves of chemiluminescence systems: (a) luminol-H₂O₂; (b)
4 luminol-H₂O₂-Au NCs. Luminol: 2.7×10^{-5} mol/L ; H₂O₂: 1×10^{-7} mol/L; Au NCs:
5 16 mg/L; pH :11.3 (sodium hydroxide solution).



6
7 **Figure2.** Chemiluminescence spectra for luminol-H₂O₂-Au NCs system. (a) Au NCs;
8 (b) luminol-H₂O₂; (c) luminol-H₂O₂-Au NCs. Luminol: 2.7×10^{-5} mol/L ; H₂O₂: $1 \times$

1
2
3
4
5
6
7
8
9
10
11
12
13
14
15
16
17
18
19
20
21
22
23
24
25
26
27
28
29
30
31
32
33
34
35
36
37
38
39
40
41
42
43
44
45
46
47
48
49
50
51
52
53
54
55
56
57
58
59
60

9 10^{-7} mol/L; Au NCs: 16 mg/L; pH 11.3 (sodium hydroxide solution).



17

18

19 **Figure3.** Effects of the reaction conditions on the luminol-H₂O₂-Au NCs CL system.

20 (a) Effects of pH of luminol: Luminol: 2.7×10^{-5} mol/L; H₂O₂: 1×10^{-7} mol/L; Au

21 NCs: 5 mg/L (b) Effect of luminol concentration: pH:11.3; H₂O₂: 1×10^{-7} mol/L; Au

22 NCs: 5 mg/L (c) Effect of Au NCs: Luminol: 2.7×10^{-5} mol/L; H₂O₂: 1×10^{-7} mol/L;

23 pH: 11.3.

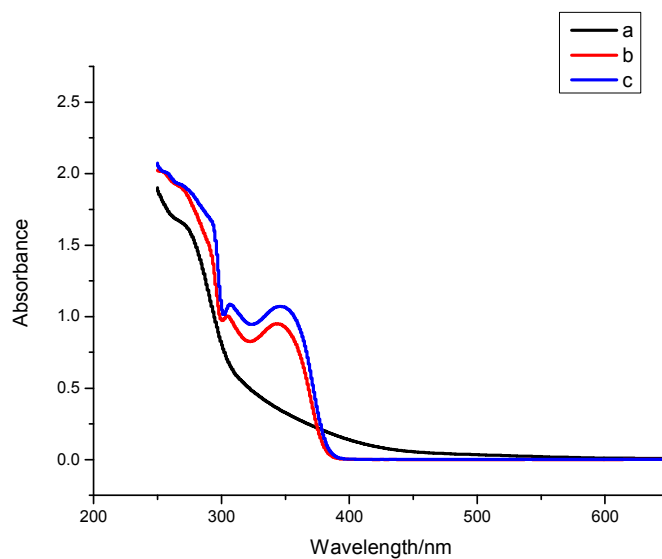
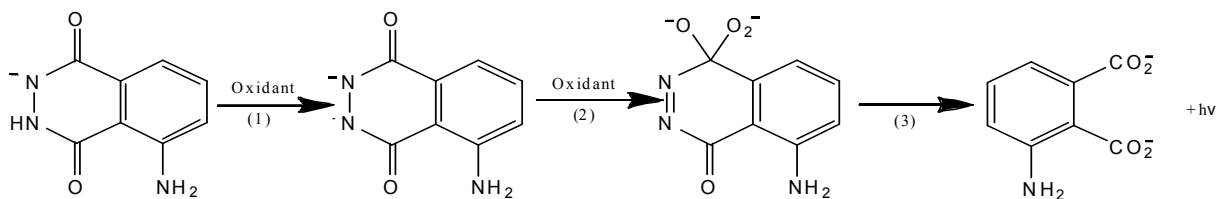
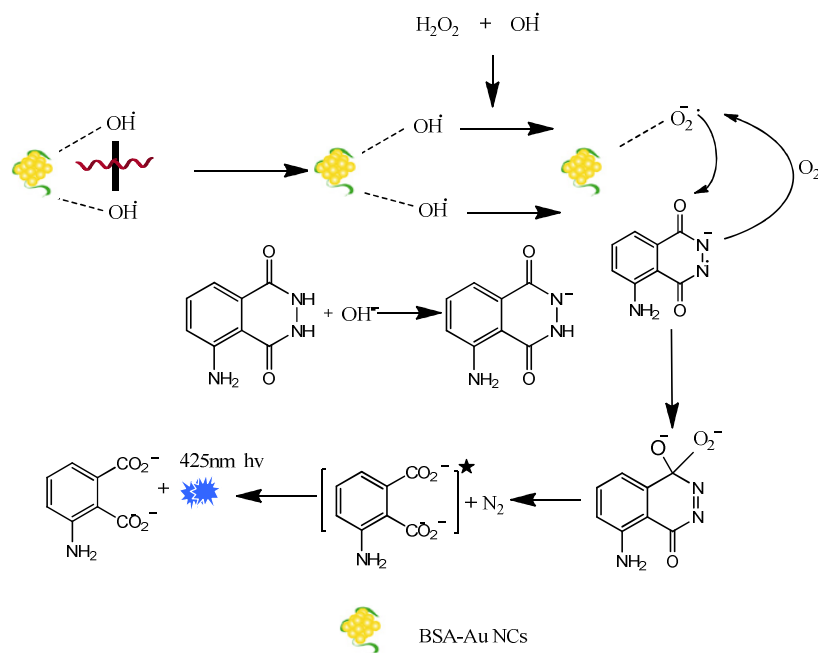


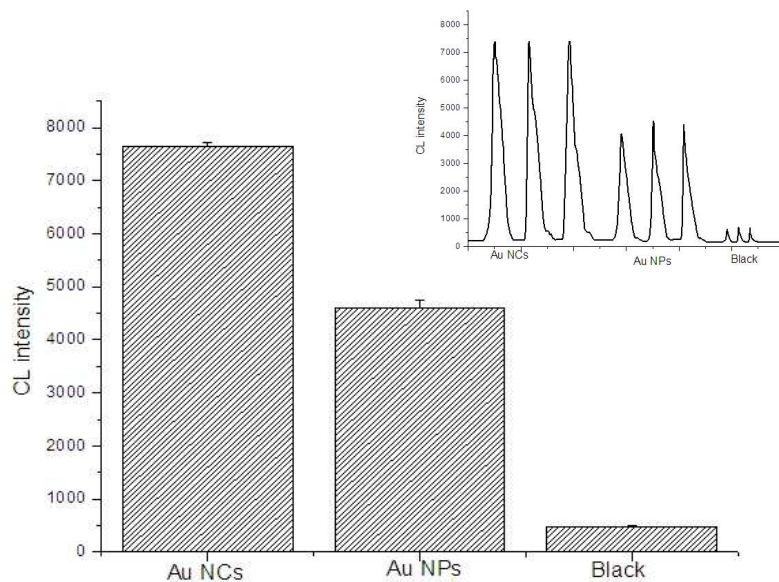
Figure 4. UV-visible absorption spectra of (a) Au NCs; (b) luminol-H₂O₂; (c) luminol-H₂O₂-AuNCs



Scheme 1. Schematic CL-generating mechanism for the oxidation of luminol with three major steps

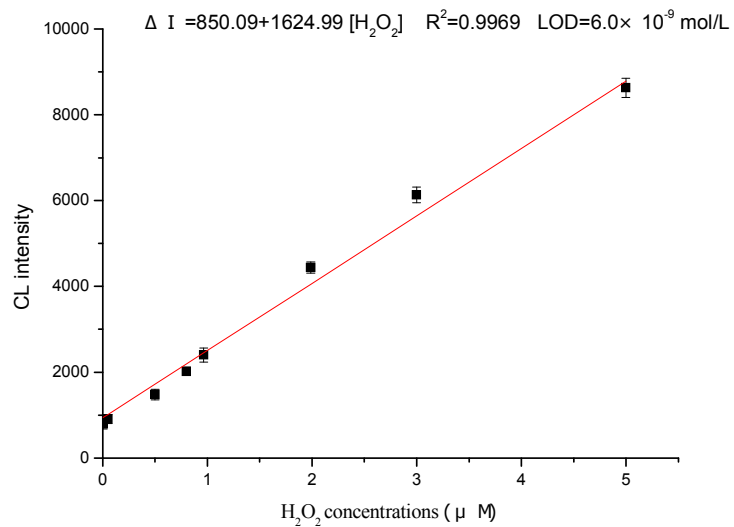


Scheme 2. Possible mechanism for the luminol-H₂O₂-Au NCs CL system.



1
2
3
4 47 **Figure5** Comparison of CL intensity in luminol-catalyzed reaction in pH 11.3, $2.7 \times$
5
6 10^{-5} mol/L luminol and 1×10^{-7} mol/L H_2O_2 . Inset: Comparison of CL intensity in
7
8
9 49 luminol-catalyzed reaction for Chemiluminescence spectra.
10

11
12
13
14
15
16
17
18
19
20
21
22
23
24
25
26
27
28
29
30
31
32



33 51

34
35 52
36
37
38

39 53
40
41
42
43
44
45
46
47
48
49
50
51
52
53
54
55
56
57
58
59
60

Figure 6. Calibration curves for H_2O_2 .

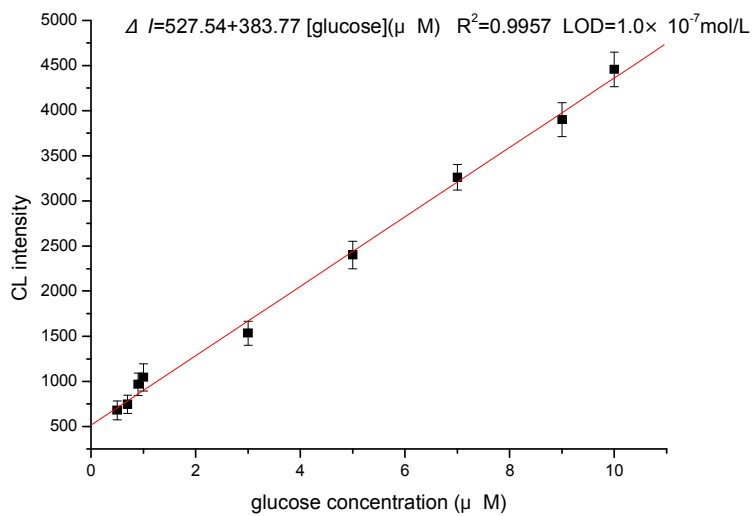


Figure 7. Calibration curves for glucose.